

INCORPORATING SET-UP AND SUPPORT COST DISTRIBUTIONS INTO DRIVEN PILE DESIGN

Van E. Komurka¹, P.E., Member, ASCE

ABSTRACT: Accounting for set-up in pile design can result in using smaller hammers, smaller pile sections, shorter piles, higher capacities/allowable loads, and therefore more-economical installations than otherwise possible. Geotechnical characterization of a pile-foundation site (anticipated driving behavior, set-up magnitude and distribution, and long-term capacity distribution), combined with installation costs for various pile options, can be used to select cost-efficient pile installations based on support cost. Support cost is the cost of the installed or constructed foundation element (or system) divided by its allowable load. Two case histories are presented: the first utilizes dynamic monitoring during initial drive and restrike testing to characterize end-of-initial-drive capacity, unit set-up, and long-term capacity distributions. Such characterizations permit development of depth-variable penetration resistance criteria. The second case history presents long-term capacity and a number of installation cost components as functions of depth, which aids in determining support cost as a function of depth for two candidate pipe pile sections. The resulting support cost distributions are used to select the most-cost-efficient pile section and allowable pile load for the structure.

INTRODUCTION

After installation, pile capacity increases with time. This time-dependent capacity increase is known as set-up, and was first mentioned in the literature in 1900 by Wendel [Long et al., 1999]. An overview of set-up is presented in Komurka et al. (2003a, 2003b). Set-up has been documented in fine-grained soils in most parts of the world [Soderberg, 1961], and has been demonstrated to account for capacity increases of up to 12 times initial [Titi and Wathugala, 1999]. Set-up rate and magnitude are functions of multiple factors [Samson and Authier, 1986], the interrelationship of which is not well understood.

Set-up is predominately associated with increased shaft resistance [Bullock, 1999; Chow et al., 1998; Fellenius et al., 2000; Lukas and Bushell, 1989], and is

¹ Vice President, Wagner Komurka Geotechnical Group, Inc., W67 N222 Evergreen Boulevard, Suite 100, Cedarburg, Wisconsin 53012, komurka@wkg2.com

primarily related to excess porewater pressure dissipation within, and subsequent remolding and reconsolidation of, soil which is displaced and disturbed as the pile is driven. Depending on permeability and amount of disturbance, excess porewater pressure dissipation can be non-uniform (non-linear with respect to the log of time) for some time after driving. Subsequently, excess porewater pressure dissipation is uniform (linear with respect to the log of time. Independent of porewater pressure change (i.e., independent of effective stress), additional set-up occurs due to aging [Camp et al., 1993; Long et al., 1999; McVay, 1999; Schmertmann, 1981; Schmertmann, 1991].

Set-up is recognized as occurring for virtually all types of driven piles, in organic silt, inorganic saturated clay, and loose to medium dense silt, sandy silt, silty sand, and fine sand. In cohesive soils, set-up is related to soil and pile properties [Camp and Parmar, 1999; Finno et al., 1989; Long et al., 1999], and the remolded soil's shear strength is higher than the soil's undisturbed shear strength [Randolph et al., 1979; Seed and Reese, 1955]. In fine-grained granular soils, set-up is related to soil and pile properties, and creep-induced breakdown of driving-induced arching mechanisms [Chow et al., 1997, 1998; Malhotra, 2002]. Since set-up is related to excess porewater pressure dissipation, the more-permeable the soil, the faster set-up develops. Set-up rate decreases as pile size increases [Long et al., 1999; Wang and Reese, 1989].

A number of empirical relationships have been proposed to estimate or predict set-up, and have demonstrated reasonable success (accuracy) in a number of studies [Skov and Denver, 1988; Svinkin, 1996; Guang-Yu, 1988; Huang, 1988; Svinkin and Skov, 2000]. Established relationships are limited in widespread application by having been based on combined (shaft and toe) resistance determinations, interdependence of back-calculated or assumed variables, and the complexity of the mechanisms contributing to set-up.

If project scope (size) justifies it, a well-designed and executed project-specific test program can yield more-valuable set-up characterization than empirical relationships. Set-up measurement requires pile capacity be determined a minimum of two times. To maximize measured set-up, a pile's first capacity determination should be performed at the end of driving, or as soon after driving as possible, and the second determination should be delayed as long as possible (i.e., as long as the project schedule permits). However, this time interval should not be longer than the time interval between production-pile installation and service load application (otherwise, there is risk of relying on set-up before it develops). Capacity determinations should separate shaft and toe resistance, and are most-valuable if unit shaft resistance distribution (unit shaft resistance as a function of depth) is determined. Such capacity determinations can be achieved with top- or bottom-loaded internally instrumented static load tests, or dynamic testing with subsequent CAPWAP analyses [Hussein et al., 2002; Likins et al., 1996; Rausche et al., 1972, 1994, 1996, 2000], or preferably both.

Pile test programs which characterize set-up only as capacity increase magnitude lack flexibility in developing or modifying production pile installation criteria. For example, if a test pile is installed, its end-of-initial-drive ("EOID") capacity is determined, and its capacity at some later time is determined to have increased, set-up

magnitude has been quantified. However, without characterization of set-up distribution as a function of depth, it is difficult (if not impossible) to determine how much shorter (if the test pile's capacity is greater than required) or longer (if the test pile's capacity is less than required) production piles should be installed to achieve desired capacity(ies).

Determination of not only set-up magnitude, but also distribution (as a function of depth), makes such determinations possible. Set-up distribution determination also provides other design- and construction-phase flexibilities such as accounting for set-up when developing installation criteria for numerous different required production-pile capacities, and more-accurate assignment of reduced capacities to short or damaged piles.

To aid in determining set-up magnitude and distribution, static load test piles can be internally instrumented to determine shaft resistance distribution, and test piles can receive restrike testing (i.e., can be restruck). The piles' potentially increased impedance (e.g., from concrete fill) notwithstanding, because of set-up, a larger hammer with greater impact force than used for initial driving may be required to mobilize the piles' capacities (move the piles) during restrike testing.

Two case histories herein present four aspects of a pile test program in Milwaukee, Wisconsin. The first case history demonstrates characterization of unit set-up distribution (unit set-up as a function of depth), and depth-variable penetration resistance criteria development, for high-capacity (190-ton allowable load) pipe piles. The second case history demonstrates characterization of support cost distributions (support cost as a function of depth), and their use in selecting the most-cost-efficient pile section and allowable load for a structure.

PROJECT DESCRIPTION

The Sixth Street Viaduct Replacement Project involved demolishing the existing Sixth Street Viaduct (which spanned the Menomonee River Valley in Milwaukee, Wisconsin), and constructing its replacement. The new viaduct alignment structure layout is essentially symmetrical north and south from an at-grade crossing at the alignment's approximate midpoint, and includes two approach embankments and two approach structures, two bascule bridges (spanning the Menomonee River, and the South Menomonee Canal), two cable-stayed bridges, and two abutments. Because of each structure's load magnitude, and the number of piles required, a pile test program was performed at each of the two bascule bridges, and at each of the two cable-stayed pylon structures.

FIRST CASE HISTORY—UNIT SET-UP DISTRIBUTION

The first case history, demonstrating unit set-up distribution characterization and depth-variable penetration resistance criteria development, presents south pylon pile test program results. The south pylon structure supports the center portion of the south cable-stayed bridge (Structure B-40-413A). The cable-stayed portion of the bridge has 195-foot-long main spans, and 115-foot-long back spans. The south pylon structure consists of two single towers, each 136 feet high and inclined 10 degrees from vertical toward the back span. The cable-stayed bridge and approaches

superstructure consists of a variable-depth concrete slab, post-tensioned longitudinally and transversely. The superstructure supports four traffic lanes, a 10-foot-wide pedestrian sidewalk, and a five-foot-wide bicycle lane. Two planes of stay-cables in a fan arrangement support the superstructure, and separate vehicular and pedestrian traffic. At each tower, design compression load is approximately 7,000 kips, with transverse and longitudinal moments approaching 20,000 foot-kips.

Subsurface Conditions

Project subsurface explorations and geotechnical evaluations were performed by others, and included performing three soil borings (Borings 1-1A, 2-2, and 2-3) in the vicinity of the south pylon structure [Giles, 2000; STS, 1999]. These borings' depths ranged from 121 to 224 feet, with corresponding bottom-of-boring elevations ranging from -107.2 to -187.6 feet (Milwaukee City Datum). The boring locations are presented in Figure 1. A schematic log of the test piles' closest boring, Boring

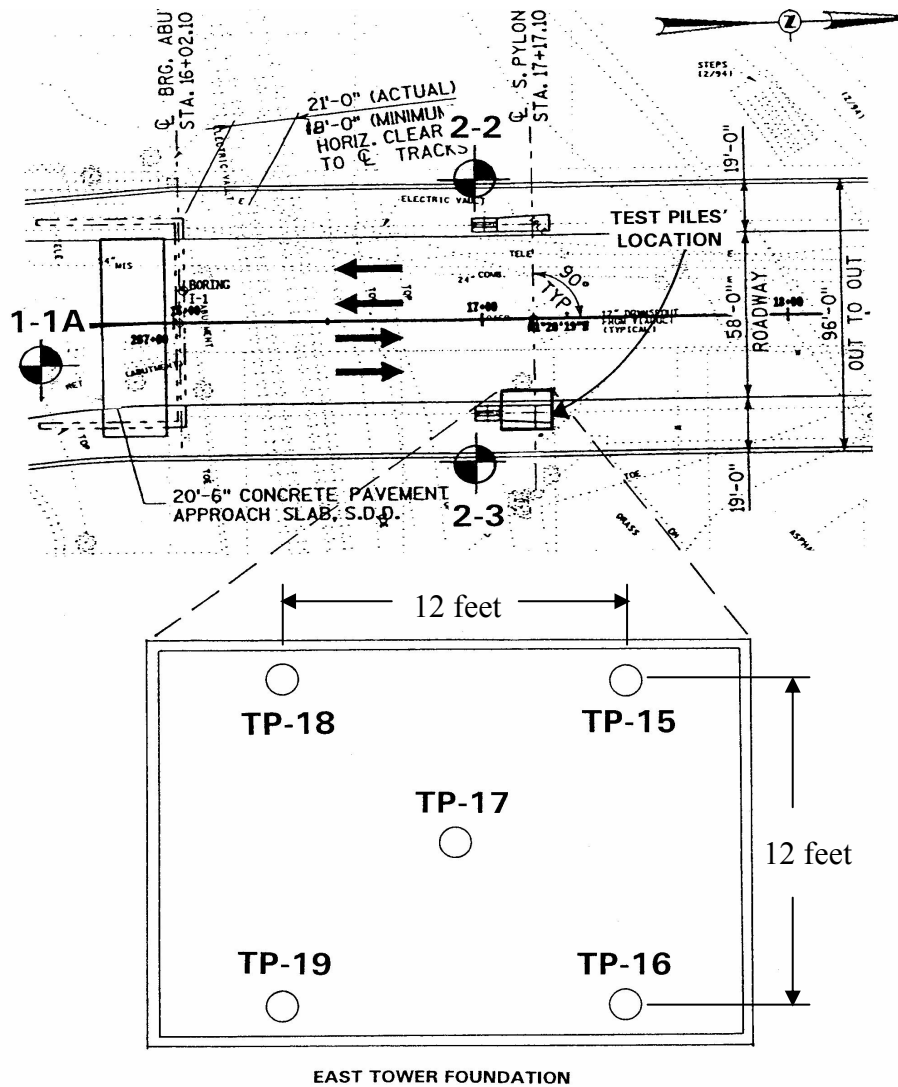


FIG. 1. Test pile location diagram.

2-3, is presented in Figure 2. Although Borings 2-2 and 2-3 were most-proximate to the south pylon structure, both borings terminated higher than the test piles. Accordingly, discussion of the conditions encountered in Boring 1-A (the nearest boring which extended as deep as the test piles) below Elevation -111.7 feet is also included.

Boring 2-2 was drilled proximate to the west tower leg; Boring 2-3 was drilled proximate to the east tower leg (the pile test program location). These two borings encountered similar subsurface profiles, including fill deposits comprised of silty clay, to fine to coarse sand, extending to elevations ranging from 7.3 to 8.3 feet, underlain by loose to medium dense fine-grained granular deposits consisting of clayey silt, to fine sand, which extended to elevations ranging from 0.8 to -18.7 feet. Underlying deposits consisted predominately of very stiff silty clay, with occasional layers of loose to medium dense clayey or sandy silt, to the termination depths of the borings (Elevations -107.2 and -111.7 feet, respectively). In both borings, cobbles and boulders were encountered in the silty clay deposits below Elevations -64.2 and -73.7 feet, respectively. Below Elevation -111.7 feet, Boring 1-A encountered very dense fine to coarse sand and gravel, with cobbles and boulders. Bedrock was encountered at Elevation -177.6 feet.

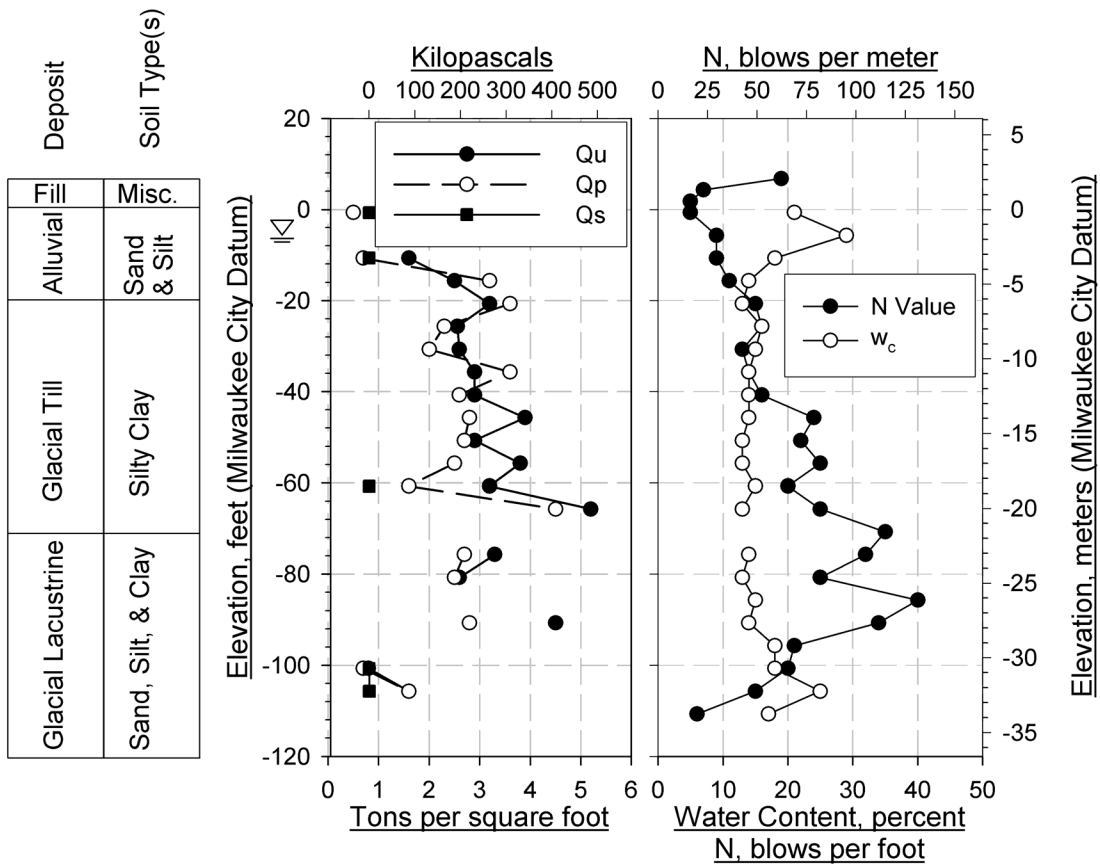


FIG. 2. Subsurface conditions, Borings 2-2 and 2-3.

Pile Test Program

Installation

General

The test piles consisted of 12.75-inch-outside-diameter steel pipe piles, with 0.375-inch-thick walls. Five test piles were installed, all in the east tower footprint (the existing viaduct alignment ran through the west tower footprint, precluding crane access). The test pile locations are presented in Figure 1.

The test piles were installed using a Delmag D30-32 single-acting diesel hammer, having a manufacturer's indicated ram weight of 6.6 kips, a manufacturer's indicated maximum stroke of 10.6 feet, and a manufacturer's maximum rated energy of 73.7 foot-kips. The hammer cushion consisted of two 1-inch-thick Micarta[®] discs, and two ½-inch-thick aluminum discs.

The test piles were driven closed-end, with a ¾-inch-thick 13.25-inch-O.D. steel boot plate. Each pile installation consisted of a bottom section, and varying numbers of upper sections. Splicing operations, and subsequent driving resumption, were considered part of initial driving. Splices were made with a full-circumference weld using a backup ring. Subsequent to initial driving, the piles were filled with concrete having a minimum 28-day design strength of 6,000 pounds per square inch (psi).

Dynamic Monitoring

Initial driving of all test piles was dynamically monitored by Goble Rausche Likins and Associates, Inc. ("GRL") of Palatine, Illinois, using a PAK model Pile Driving Analyzer[®] ("PDA") instrumentation system. The PDA instrumentation system has been described by others [Hussein and Likins, 1995; Likins et al., 2000; Rausche et al., 1985].

Additional analysis of field-measured dynamic monitoring data included performing a **C**ase **P**ile **W**ave **A**nalysis **P**rogram ("CAPWAP[®]") analysis on a representative blow from each test pile's EOID. CAPWAP analyses have been described by others [Hussein et al., 2002; Likins et al., 1996; Rausche et al., 1972, 1994, 1996, 2000].

All EOID CAPWAP analyses were performed using the residual stress analysis ("RSA") option [Pile Dynamics, Inc., 1998]. For long, flexible piles which develop a significant portion of their capacity in shaft resistance, this analysis option is preferred because it judiciously accounts for residual compression stress which can be locked into the pile shell by shaft resistance during driving. Accounting for this locked-in stress is essential for proper static load test strain gage data interpretation, and for proper calculation of toe and shaft resistance. A CAPWAP analysis using the RSA option can result in prediction of less shaft resistance, and more toe resistance, than a non-RSA analysis. However, a CAPWAP analysis using the RSA option predicts the same total (toe plus shaft) pile resistance as a non-RSA analysis (i.e., only the division of resistance between the toe and shaft may vary).

The PDA data and subsequent CAPWAP analyses were used to determine pile capacities, the division of capacity between toe and shaft resistance, and shaft resis-

tance distribution. The PDA data also provided information on dynamic soil parameters, pile stresses, and hammer performance.

Restrike Testing

General

Unit set-up determination is typically appropriate for discrete pile sections, such as pile sections between strain-gage elevations for static load-test data, or some fraction of total pile length for CAPWAP analyses. Unit set-up for a particular pile segment is defined as the shaft resistance increase attributable to set-up for that pile segment, divided by the surface area of that pile segment.

Restrike testing was performed 69 to 70 days after EOID using a Delmag D36-32 single-acting diesel hammer, having a manufacturer's indicated ram weight of 7.93 kips, a manufacturer's indicated maximum stroke of 10.6 feet, and a manufacturer's maximum rated energy of 88.5 foot-kips. The hammer cushion consisted of two 1-inch-thick Micarta discs, and two ½-inch-thick aluminum discs. In addition, a pile cushion consisting of a ¾-inch-thick plywood disc was used. A new plywood pile cushion was used for each test pile's restrike. Test Pile TP-17 had been statically load tested prior to restrike.

Dynamic Monitoring

Restrike testing of all test piles was monitored by GRL using a PDA. Additional laboratory analysis of field-measured dynamic monitoring data included performing a CAPWAP analysis on a representative blow from each pile's beginning-of-restrike ("BOR") testing. As with EOID CAPWAPs, all BOR CAPWAPs were performed using the residual stress analysis option.

Results and Analysis

Select pile test program results are summarized in Table 1.

Installation

The test piles' driving behavior is presented as a plot of penetration resistance versus (vs.) elevation in Figure 3; the average penetration resistance vs. elevation is also included in Figure 3.

Since the test piles were installed using a variable-stroke hammer, and since the penetration resistances presented in Figure 3 do not account for variations in stroke, the penetration resistances are not directly comparable to each other. A more-direct comparison of driving behavior can be made using Case Method initial-drive capacities estimated by the PDA based on dynamic monitoring results. Case Method capacity determination from dynamic monitoring results has been described by others [Goble et al., 1975; Hannigan, 1997; Pile Dynamics, Inc., 1998; Rausche et al., 1985]. Essentially, for every foot of driving, the PDA estimates an average capacity (i.e., estimates the EOID capacity the pile would have if driving had stopped at any

Table 1. Pile test program data summary.

Test Pile (1)	Driving Status (2)	Time After Initial Drive, days (3)	Penetration Depth, feet (4)	Toe Elevation, feet (5)	Penetration Resistance, blows / inches (6)	Equivalent Penetration Resistance, blows/foot (7)	Mobilized Capacity, kips			Capacity Fully Mobilized? (11)
							Shaft (8)	Toe (9)	Total (10)	
TP-15	EOID	---	136.4	-127.6	19 / 1	228	58	380	438	No
	BOR	69	136.4	-127.6	6 / 0.5	144	322	378	700	No
TP-16	EOID	---	135.1	-126.3	18 / 1	216	57	365	422	No
	BOR	69	135.1	-126.3	8 / 0.5	192	407	355	762	No
TP-17	EOID	---	130.0	-121.2	7 / 1	84	90	331	421	Yes
	SLT	64	130.0	-121.2	---	---	724	220	944	Yes
	BOR	69	130.0	-121.2	9 / 0.5	216	371	455	826	No
TP-18	EOID	---	131.0	-122.2	80 / 12	80	62	290	352	Yes
	BOR	69	131.0	-122.2	5 / 0.5	120	357	320	677	No
TP-19	EOID	---	115.3	-106.5	11 / 4	33	130	69	199	Yes
	BOR1	0.7	115.3	-106.5	11 / 1	132	178	290	468	No
	BOR2	70	115.7	-106.9	10 / 0.5	240	463	310	773	No

Conversion to SI units
 1 foot = 0.3048 m
 1 kip = 4.448 x 10³ N

given depth). A Case Method damping factor of 0.90 (RX9, i.e., $J=0.9$) was used for these initial-drive capacity estimates. These data are presented as a plot of initial-drive Case Method capacities vs. elevation in Figure 4; the average initial-drive Case Method capacity vs. elevation is also included in Figure 4.

A review of Figure 4 indicates that the indicator piles exhibited similar initial-drive capacities to elevations on the order of -50 to -60 feet, below which TP-16, TP-17, and TP-19 showed considerably higher initial-drive capacities than TP-15 and TP-18 (TP-15 and TP-18 were the westernmost piles). At elevations ranging from -120 to -125 feet, the piles exhibited similar increases in initial-drive capacity.

As presented in Table 1, the test piles' embedded depths ranged from 115.7 to 136.4 feet (with corresponding toe elevations ranging from -106.9 to -127.6 feet), with EOID equivalent penetration resistances ranging from 33 to 228 blows per foot (bpf). Also as presented in Table 1, TP-15 and TP-16 had high enough EOID penetration resistances (greater than approximately 10 blows per inch) to indicate that their full capacity was not mobilized, particularly at or near the toe [Hannigan et al., 1997]. CAPWAP-calculated EOID capacities ranged from 100 to 219 tons; CAPWAP-calculated EOID shaft resistances ranged from 29 to 65 tons.

CAPWAP analyses estimated the test piles' EOID unit shaft resistance distributions. The CAPWAP-determined EOID unit shaft resistance distributions are presented as plots of unit shaft resistance vs. elevation in Figure 5; the average EOID unit shaft resistance distribution (sans TP-19) vs. elevation is also included in Figure 5. A review of Figure 5 indicates that, with the exception of TP-19, the EOID unit shaft resistance distributions are similar to each other.

Static Loading Test

The load-movement curve for the static loading test is presented in Figure 6. Based on the Davisson Offset Limit criterion [Davisson, 1973], the pile was assigned a capacity of 472 tons.

Restrike Testing

As presented in Table 1, BOR equivalent penetration resistances ranged from 120 to 240 bpf. Also as presented in Table 1, with the exception of TP-18, the test piles had high enough BOR penetration resistances to indicate that their full capacity was not mobilized. TP-18's full capacity may or may not have been mobilized. CAPWAP-calculated BOR capacities ranged from 338 to 413 tons; CAPWAP-calculated BOR shaft resistances ranged from 161 to 232 tons.

For TP-17 which was statically load tested, CAPWAP predicted a capacity of 413 tons vs. 472 tons determined from the static loading test, an underprediction of 59 tons, corresponding to 12 percent of the static-loading-test-determined capacity. TP-17 had a BOR penetration resistance of 216 bpf, indicating its full capacity was not mobilized during restrike.

CAPWAP analyses also predicted the test piles' BOR unit shaft resistance distributions. The CAPWAP-determined BOR unit shaft resistance distributions are presented as plots of unit shaft resistance vs. elevation in Figure 7; the average BOR unit shaft resistance distribution determined from CAPWAP analyses (sans TP-19)

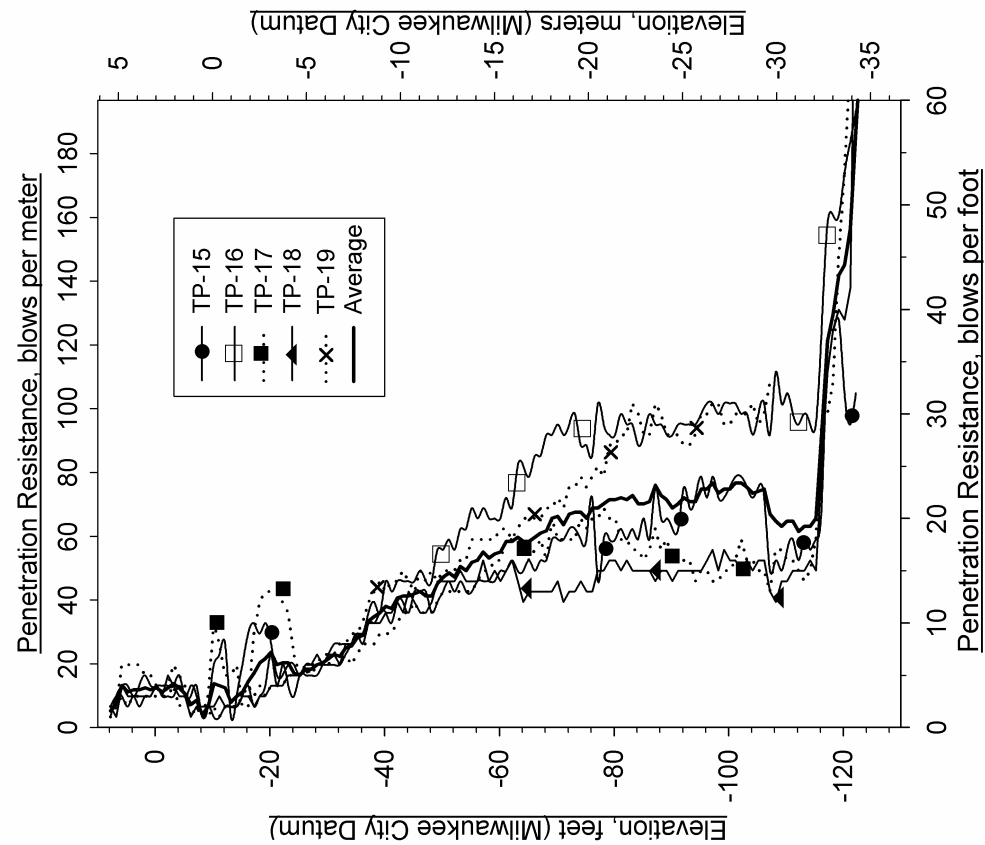


FIG. 3. Penetration resistance vs. elevation.

Note: Piles were driven in the following order: TP-19, -18, -16, -15, -17.

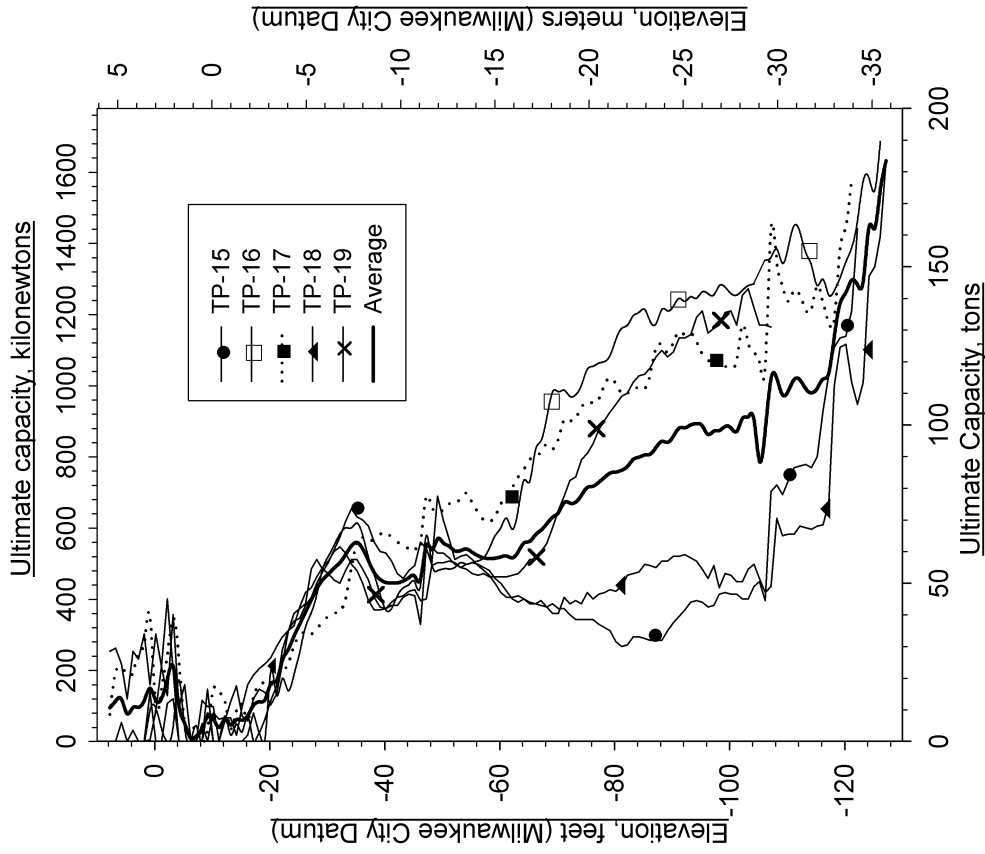


FIG. 4. Initial-drive Case Method capacity vs. elevation.

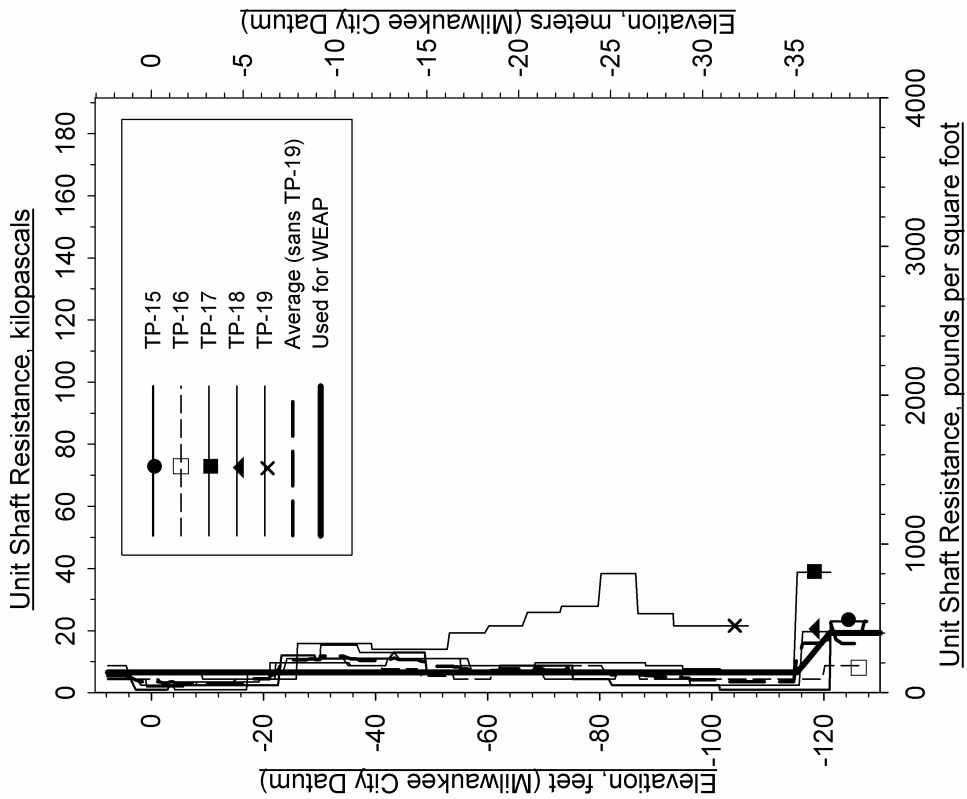


FIG. 5. EOID CAPWAP unit shaft resistance vs. elevation.

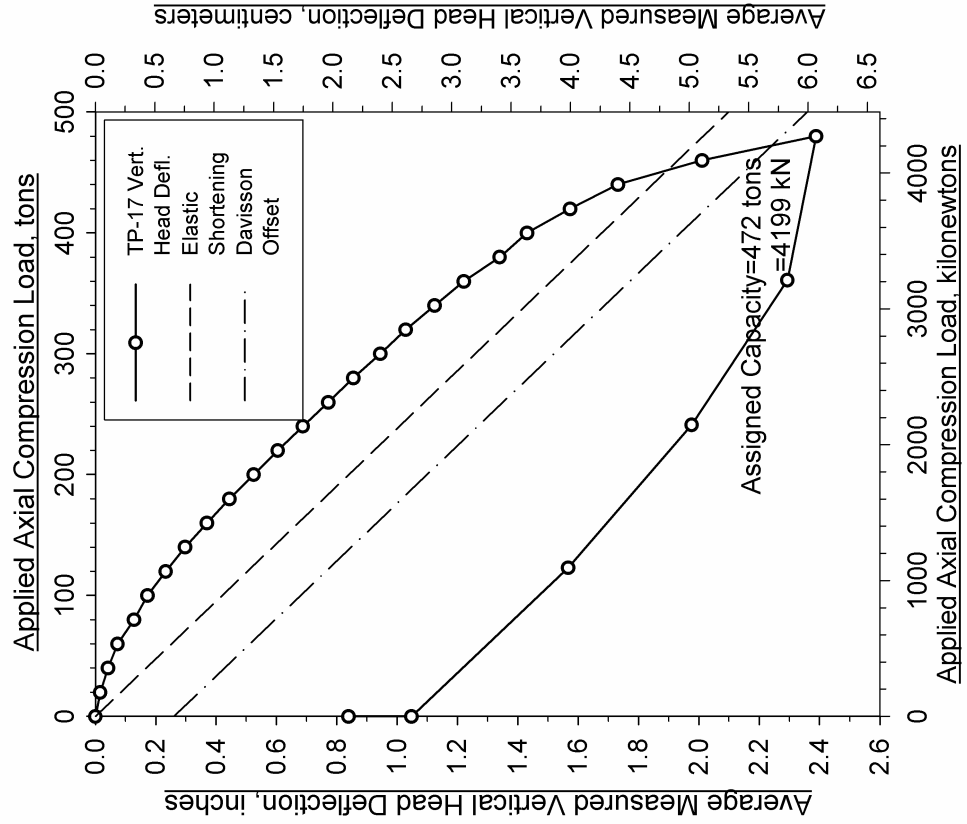


FIG. 6. Static load test pile (TP-17)—measured vertical head deflection vs. applied axial compression load.

vs. elevation is also included in Figure 7. A review of Figure 7 indicates that, with the exception of TP-19, the BOR unit shaft resistance distributions show relatively good correlation with each other.

To allow for comparison with dynamic monitoring data, 10 internal vibrating wire strain gages (Geokon Model 4911 “sister bars”) provided information on load-transfer behavior and unit shaft resistances for TP-17 during the static loading test. These data were adjusted for residual stresses as determined by TP-17’s EOID CAPWAP [Fellenius, 2001a, 2001b, 2001c, 2002]. In general, static-load-test determined unit shaft resistances showed good agreement, to slight overprediction (as would be expected), compared to unit shaft resistances predicted by TP-17’s BOR CAPWAP.

Set-Up

CAPWAP-determined unit set-up distributions were calculated for each test pile by subtracting the EOID CAPWAP-determined unit shaft resistance distribution from the BOR CAPWAP-determined shaft resistance distribution (i.e., by subtracting the values presented in Figure 5 from those presented in Figure 7). For each pile, since an EOID unit shaft resistance distribution is subtracted from a BOR unit shaft resistance distribution, the accuracy of the resulting difference (the unit set-up distribution) is sensitive to the accuracy of both the EOID and BOR unit shaft

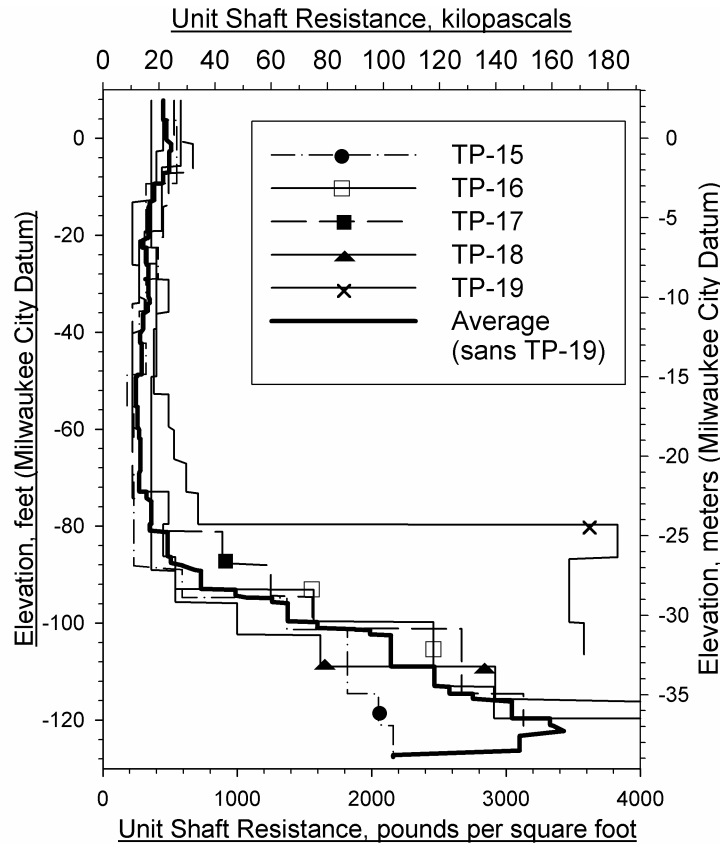


FIG. 7. BOR CAPWAP unit shaft resistance vs. elevation.

resistance distribution. If either the EOID or BOR unit shaft resistance distribution is underestimated because the pile's capacity was not fully mobilized (i.e., the penetration resistance was too high), the accuracy of the calculated unit set-up distribution is compromised.

If both EOID and BOR capacity are fully mobilized, set-up is determined to a reasonable degree of accuracy. If EOID capacity is fully mobilized but BOR capacity is not fully mobilized, set-up is underestimated. If EOID capacity is not fully mobilized but BOR capacity is fully mobilized, set-up is overestimated (it may be possible to rectify this situation by performing a CAPWAP analysis on an earlier initial-drive blow). If neither EOID nor BOR capacity is fully mobilized, the effect on the accuracy of set-up determination is uncertain. These scenarios are illustrated in Table 2, along with each of the test piles' situation among these scenarios. A review of Table 2 indicates that with the exception of TP-18, the test piles' unit set-up distributions were either underpredicted, or indeterminate. TP-18's full capacity may or may not have been mobilized, so its unit set-up prediction was either reasonably accurate, or was underpredicted.

The CAPWAP-determined unit set-up distributions are presented as plots of unit set-up vs. elevation in Figure 8; the average unit set-up distribution (sans TP-19) vs. elevation is also included in Figure 8. The test piles' unit set-up distributions being either reasonably accurate, underpredicted, or indeterminate notwithstanding, a review of Figure 8 indicates that, with the exception of TP-19, the CAPWAP-determined unit set-up distributions show relatively good correlation with each other. A review of Figure 8 indicates that the indeterminate unit set-up distributions (TP-15 and TP-16) were similar to, or less than, those which were reasonably accurate and those which were underpredicted (TP-17, TP-18, and TP-19). A comparison of Figures 4 and 8 indicates that there is better correlation among the unit set-up distributions than among the initial-drive Case Method capacities.

Table 2. Relationships between EOID and BOR capacity mobilization and set-up determination.

		BOR Capacity	
		Fully Mobilized	Not Fully Mobilized
EOID Capacity	Fully Mobilized	Set-Up Reasonably Accurate TP-18 ?	Set-Up Underpredicted TP-17 TP-18 ? TP-19
	Not Fully Mobilized	Set-Up Overpredicted	Set-Up Indeterminate TP-15 TP-16

Application to Design and Installation

Wave-Equation Input Parameters

The wave equation program GRLWEAP™ was used to evaluate driving stresses and potential EOID capacities associated with using a different hammer for production piles than was used to install the test piles, and to generate production pile penetration resistance criteria. GRLWEAP has been described by others [Hussein et al., 1988; Thendean, 1996]. A number of test pile program results were applied to the wave equation analyses.

EOID Shaft Resistance Distribution

The average unit shaft resistance distribution determined from the test piles' EOID CAPWAPs, as presented in Figure 5, was used in the GRLWEAP analyses.

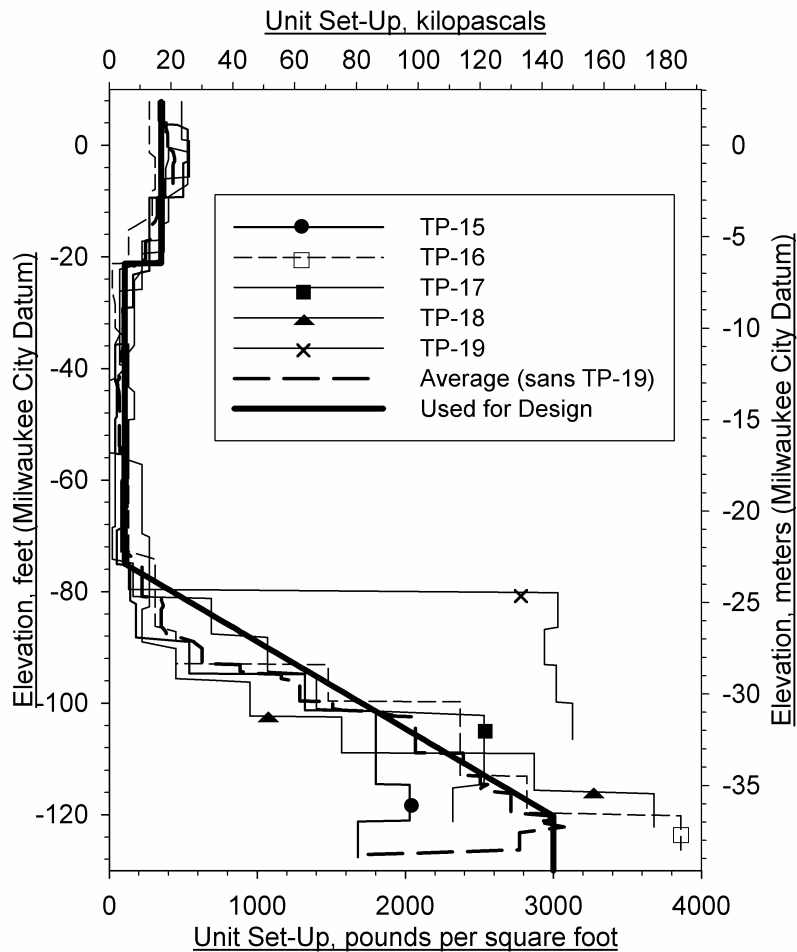


FIG. 8. EOID/BOR CAPWAP unit set-up vs. elevation.

Refined Input Parameters

For each test pile, a number of GRLWEAP's input parameters were back-calculated based on the results of EOID CAPWAPs, resulting in refined wave equation analyses. GRLWEAP input parameters of hammer efficiency, toe quake, and shaft and toe damping were systematically varied until GRLWEAP-predicted values closely matched field- and CAPWAP-determined values of capacity, penetration resistance, transferred energy, and maximum stress [Hannigan et. al., 1997]. These refined input parameters, which were used in GRLWEAP to generate production pile penetration resistance criteria, are presented in Table 3. Since TP-19 terminated shorter and with different EOID conditions (soil and driving behavior) than anticipated for production piles, the boxed values in Table 3 were used in GRLWEAP to generate production pile penetration resistance criteria.

Unit Set-Up Distribution Used for Design

The unit set-up distribution used for design is presented in Figure 8. Its application to design is discussed in the following sections.

Allowable Loads Available for Production Piles

The pile test program data were gathered and evaluated as ultimate values (ultimate unit shaft resistances, unit set-ups, and capacities). Given the amount of field testing performed and data acquired for the south pylon structure, design incorporated a minimum factor of safety of 2.0.

For a given toe elevation, the capacity to which piles can be installed is the sum of two components: initial-drive capacity (e.g., as presented in Figure 4), plus set-up. It follows that to aid in estimating long-term capacities to which production piles could be installed, initial-drive capacity and set-up can be added. The result of such an evaluation for the piles the same as the test piles, and installed using the same hammer as the test piles, is presented in Figure 9. The cumulative set-up curve in Figure 9 was obtained by applying the unit set-up distribution used for design presented in Figure 8 to the surface area of a 12.75-inch-O.D. pipe pile. A review of Figure 9 indicates that piles terminating at approximate Elevations -117 and -123 feet would attain 50 percent of their long-term capacity from set-up.

A review of Figure 9 indicates that within the maximum depth explored by the test piles, dynamic monitoring results indicate that 12.75-inch-O.D. production piles installed using a hammer similar to that used for the test program (a Delmag D30-32) could achieve long-term capacities of approximately 345 tons (of which 160 tons, or 46 percent, is set-up), resulting in potential allowable loads on the order of 172 tons. A review of Table 1 indicates that full capacity was not mobilized for any of the test piles during restrrike testing. As presented in Table 2, the test piles' unit set-up distributions were either reasonably accurate, underestimated, or indeterminate. A review of Figure 8 indicates that the indeterminate unit set-up distributions (TP-15 and TP-16) were similar to, or less than, those which were reasonably accurate, and those which were underpredicted. Accordingly, the values of capacity, set-up magnitude and percentage, and associated potential allowable loads presented in

Table 3. Refined GRLWEAP parameters.

Test Pile	Field-Measured/CAPWAP-Determined EOID Values					Refined GRLWEAP Input Parameters						
	Shaft Resistance, Percent (1)	Computed Hammer Stroke, ft (2)	Penetration Resistance, ft (3)	Transferred Energy, ft-kips (4)	EOID Capacity, kips (5)	Maximum Compression Stress, ksi (6)	D30-32 Hammer Efficiency (7)	Quake Shaft (8)	Quake Toe (9)	Damping Shaft (10)	Damping Toe (11)	Damping (12)
TP-15	13.2	8.9	228	36.9	438	32.0	0.534	0.150	0.143	0.079	0.007	
TP-16	13.5	8.9	216	37.2	422	31.6	0.551	0.140	0.182	0.132	0.018	
TP-17	21.4	9.2	84	43.0	421	35.1	0.725	0.150	0.524	0.208	0.023	
TP-18	17.6	8.4	80	40.3	352	32.8	0.665	0.140	0.494	0.360	0.043	
TP-19	65.3	7.8	33	30.5	199	32.8	0.645	0.080	1.509	0.708	0.048	
	26.2			Averages			0.624	0.132	0.570	0.297	0.028	
	16.4			Averages sans TP-19			0.619	0.145	0.336	0.195	0.023	

Conversion to SI Units
 1 ft = 0.3048 m
 1 ft-kip = 1.356 x 10³ N-m
 1 kip = 4.448 x 10³ N
 1 ksi = 6.895 MPa

Figure 9 are likely conservative (lower than actual).

For the south pylon structure, it was desired to install production piles to as high an allowable load as practical. Using GRLWEAP, the drivability of higher-capacity production piles of the same pile section as the test piles, but using a Delmag D36-32 hammer (used for test pile restrikes), was evaluated. It was determined that the larger hammer could mobilize enough additional capacity at EOID without overstressing the piles that, when combined with set-up, a long-term capacity of 380 tons was achievable, resulting in a production-pile allowable load of 190 tons.

Penetration Resistance Criteria

Subsequent to EOID, a pile’s capacity increase attributable to set-up is a function of the embedded side area of the pile, and the unit set-up distribution. The greater a pile’s embedment length, the more set-up it develops, and the less EOID capacity is required. For example, consider a pile which has a required capacity of 160 tons. At an embedded depth of 40 feet, if the pile develops 20 tons of set-up, it requires an EOID capacity of 140 tons. If the same pile driven to an embedded depth of 80 feet develops 50 tons of set-up, it requires an EOID capacity of 110 tons, and so on with increasing embedment depths.

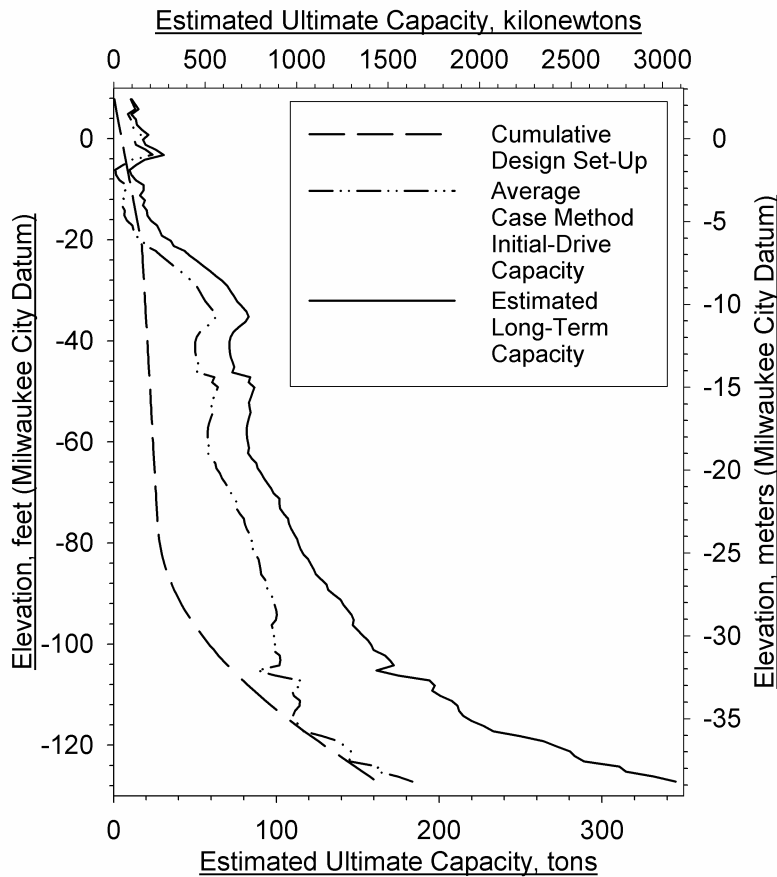


FIG. 9. Estimated ultimate capacity vs. elevation Delmag D30-32—12.75-inch pipe.

In this way, as required EOID capacity decreases with increasing embedment depth, so does required penetration resistance. Accordingly, the cumulative set-up distribution for 12.75-inch-O.D. pipe piles presented in Figure 9 was used to develop depth-variable production-pile penetration resistance criteria which decrease with increasing embedment depth. These criteria are presented in Table 4.

Depth-variable penetration resistance criteria account for both variable driving behavior of individual piles (EOID capacity as evidenced by penetration resistance, which may vary with depth and by location), and the variability of set-up with depth (set-up distribution). As a result, production piles are more-likely to be installed to realistic depths required to develop requisite capacity than with criteria which does not incorporate set-up in this way. This approach also allows flexibility in addressing such design- and construction-phase issues as developing depth-variable installation criteria for numerous (different) production-pile capacities, and more-accurate assignment of reduced capacities to short or damaged piles (which may preclude installing a replacement pile).

Production-Pile Installations

The 190-ton (allowable load) production piles driven for the two south pylon structure towers had an average embedded depth of 123 feet, corresponding to an average toe elevation of -119 feet. Ignoring pile-cap costs, the two south pylon structure towers' 190-ton production piles had an average pile support cost of \$13.92 per allowable ton supported when installed in June, 2001 (support cost is the cost of the installed or constructed foundation element or system divided by its allowable load). At this location, the relatively deep embedment depths required to reach

Table 4. Minimum required production-pile penetration resistance criteria.

Pile: 12.75x0.375		Hammer: D36-32		Allowable Load: 190 tons									
Pile Toe Depth, feet		Minimum Required Penetration Resistance, blows per foot										Pile Toe Elevation, feet	
		Hammer Stroke, feet											
from	to	6	6.5	7	7.5	8	8.5	9	9.5	10	from	to	
(1)	(2)	(3)	(4)	(5)	(6)	(7)	(8)	(9)	(10)	(11)	(12)	(13)	
115.3	117.3										—	-112	-114
118.3	120.3							—	—	—	137	-115	-117
121.3	123.3			—	—	—	139	102	80	65	-118	-120	
124.3	126.3	—	—	136	97	76	61	51	44	39	-121	-123	
127.3	129.3	110	75	58	48	41	36	32	29	26	-124	-126	
130.3	132.3	49	40	34	30	27	25	22	21	19	-127	-129	
133.3	135.3	30	26	23	21	19	18	17	16	15	-130	-132	
136.3	138.3	20	18	17	15	14	14	13	12	12	-133	-135	
139.3	141.3	15	14	13	12	11	11	10	10	10	-136	-138	
142.3	144.3	12	11	10	10	9	9	9	8	8	-139	-141	
145.3	147.3	9	9	9	8	8	8	8	7	7	-142	-144	

Conversion to SI Units: 1 ft = 0.3048 m 1 ton = 8.896 x 10³ N

strata which provided high EOID capacities tended to increase pile support costs, while the high EOID capacities to which the piles were installed, and set-up's contribution to required capacities, tended to decrease pile support costs.

SECOND CASE HISTORY—SUPPORT COST DISTRIBUTION

Introduction

Support cost provides a normalized measure of a foundation element's or system's cost-effectiveness, and affords direct "apples-to-apples" economic comparison between technically feasible foundation alternatives. It can be used to select among foundation types (e.g., shallow (spread-footing) vs. deep), among deep foundation systems (e.g., drilled pier vs. driven pile), or among design options for a given foundation type (e.g., section and capacity for driven piles). For accurate support cost determinations, all foundation system cost components should be included. For example, for pile foundation systems, the cost of the piles, as well as the cost of pile-supported structural elements whose design is a function of allowable pile load/spacing (pile caps, grade beams, wall foundations, structural floor slabs, mat foundations, etc.), should be included.

In general, experience in the Milwaukee, Wisconsin area demonstrates lower support costs for higher-capacity pile foundation systems than for lower-capacity pile foundation systems. This results from higher-capacity piles themselves generally having lower (pile) support costs, combined with lower pile-cap support costs associated with higher-capacity piles (higher-capacity piles generally require smaller, less-expensive pile caps). It should be noted, however, that although higher-capacity piles result in lower pile and pile-cap support costs, the use of higher-capacity piles where unwarranted by structure loads results in higher-than-necessary structural load support costs (the cost of the supporting foundation element(s) divided by the structural load(s) it (they) support(s)).

The second case history, demonstrating support cost distribution development and selection of the most-cost-effective pile section and allowable load for a project structure, presents results from the south bascule bridge pile test program. The south bascule bridge (Structure B-40-413B) is a trunnion-type, double-leaf, with steel superstructure on concrete piers. The superstructure is 81 feet out-to-out, providing two 12-foot traffic lanes, and a 5-foot shoulder, in each direction, plus two 10-foot-wide sidewalks. The bridge span is 134 feet from trunnion to trunnion over an 80-foot-wide channel. Each leaf of the superstructure includes two welded-plate bascule girders spaced at 58 feet center-to-center. The deck consists of floorbeam, stringer framing, which supports an open steel grid deck riding surface. The bridge is balanced with a concrete counterweight housed inside the pier. The piers are reinforced concrete, supported on concrete-filled steel pipe piles. The piers' design compression loads range from approximately 10,885 to 11,022 kips, with transverse and longitudinal moments of up to 32,338 foot-kips.

Subsurface Conditions

Project subsurface explorations and geotechnical evaluations were performed by others, and included drilling two soil borings (Borings 2-8 and 2-9) in the vicinity of

the south bascule bridge's north pier [Giles, 2000]. The boring locations are presented in Figure 10. Both borings' maximum depth explored was 121 feet (Elevation -123 feet). A schematic log of the test piles' closest boring, Boring 2-8, is presented in Figure 11. Boring 2-8 was drilled from a barge in the South Menomonee Canal, and encountered 17 feet of water (to Elev. -19 feet). Nine feet of very soft organic silty clay extended to Elev. -28 feet, underlain by 29 feet of very soft to soft organic silty clay, to clayey silt, to Elev. -57 feet. Beneath the organic soils, the boring encountered medium dense fine to coarse sand to Elev. -65 feet, underlain by 10 feet of medium to hard silty clay to Elev. -75 feet. Underlying deposits consisted of 40 feet of dense to very dense fine to coarse sand, with cobbles and boulders, to Elev. -115 feet, and 8 feet of stiff to hard silty clay to Elev. -123 feet.

Pile Test Program

A pile test program was performed at the south bascule bridge similar to the one performed at the south pylon structure (as described previously in the first case history), using the same closed-end test pile section, the same number of test piles in the same general layout, the same hammers for installation and restrrike testing, and the same dynamic monitoring, CAPWAP analyses, static load testing, and set-up determination methodology. The test pile locations are presented in Figure 10. Also similar to the first case history, the average initial-drive Case Method capacity distribution was added to cumulative set-up to aid in estimating capacities to which production piles could be installed.

12.75-Inch-Diameter Pipe Piles

The result of this evaluation for the same type piles as the test piles (12.75-inch pipe piles), and installed using a hammer similar to that used for the test program (a Delmag D30-32), is presented in Figure 12. A review of Figure 12 indicates that piles terminating at approximate Elevation -141 feet would be expected to attain their maximum percentage of long-term capacity contribution from set-up, approximately 71 percent (170 of 239 tons).

A review of Figure 12 indicates that within the maximum depth explored by the test piles, dynamic monitoring results indicate that 12.75-inch-O.D. production piles installed using a hammer similar to that used for the test program could achieve long-term capacities on the order of 400 tons (of which 186 tons, or 46 percent, is set-up), resulting in potential allowable capacities on the order of 200 tons. Full capacity was not definitively mobilized for all test piles during restrrike testing, resulting in the piles' unit set-up distributions being either reasonably accurate, or underestimated. Accordingly, set-up magnitude and percentage, and estimated long-term capacity, presented in Figure 12 are likely reasonably accurate, or conservative (lower than actual).

10.75-Inch-Diameter Pipe Piles

A review of Figure 12 indicates multi-layered subsurface profile effects, in which long-term pile capacity increases as a pile encounters a relatively competent layer (which provides increased toe resistance), then decreases as the pile advances be-

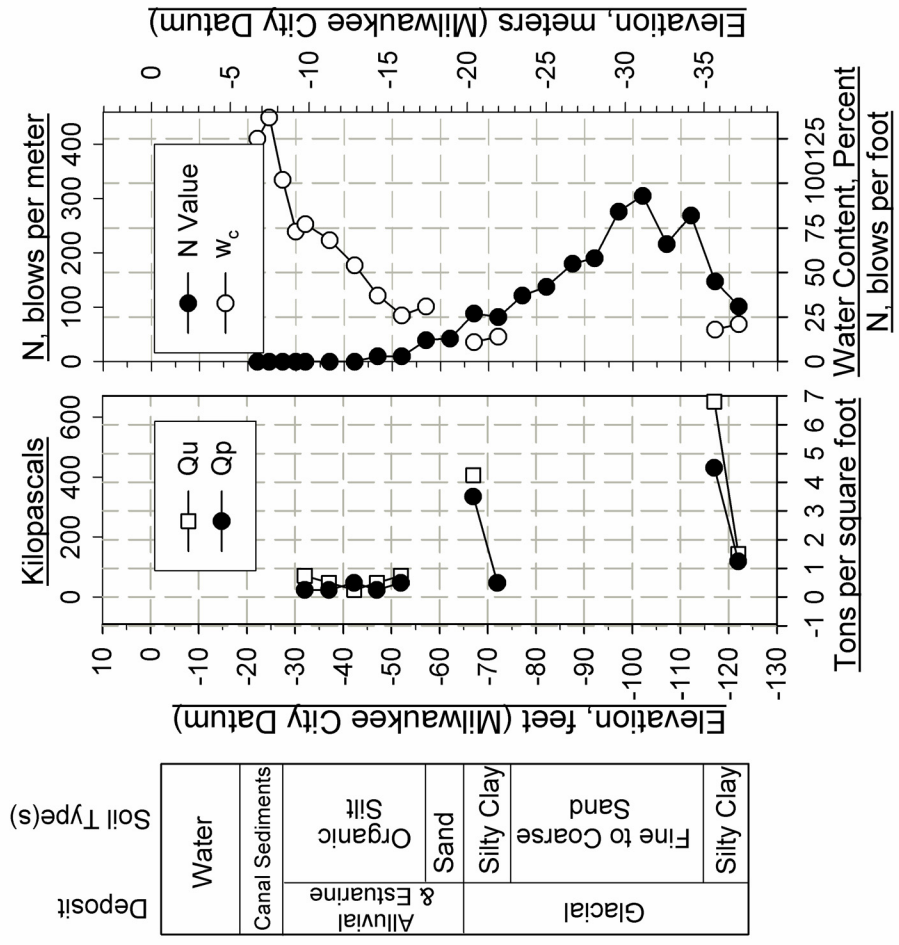


FIG. 11. Subsurface conditions, Boring 2-8.

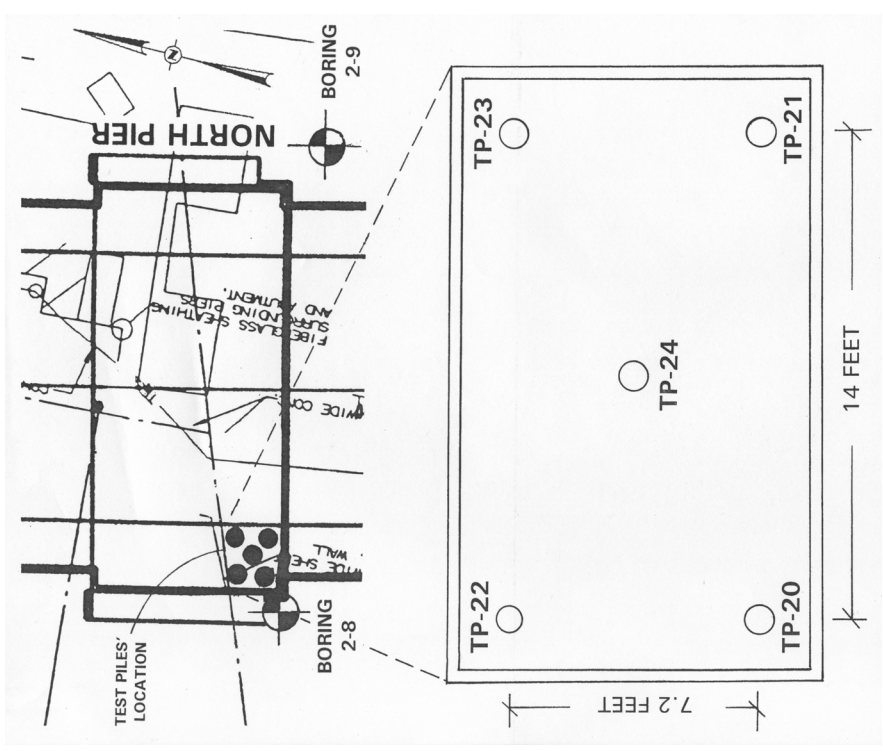
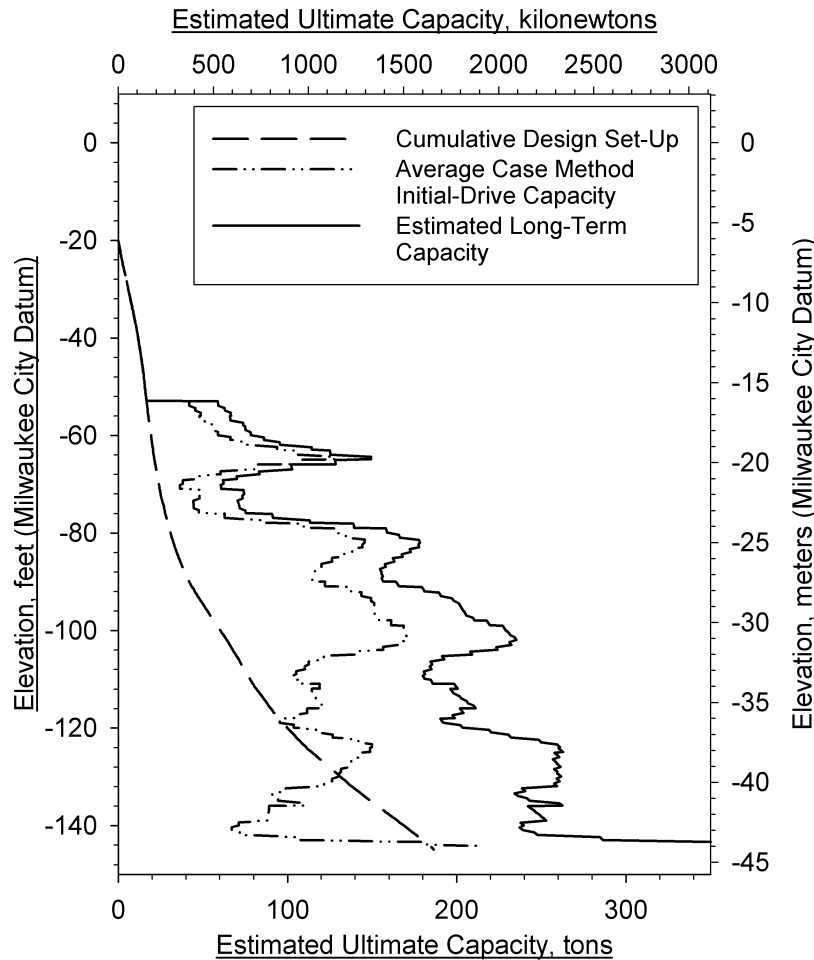


FIG. 10. Test pile location diagram.



**FIG. 12. Estimated capacity vs. elevation
Delmag D30-32—12.75-inch pipe pile.**

yond the layer into less-competent material below. Within the depth explored by the test piles, this “stratified” behavior is exhibited several times.

Elsewhere on the project, production piles consisting of 10.75-inch-O.D. steel pipe piles, with 0.250-inch-thick walls, were being installed closed-end, with a ¾-inch-thick 11.25-inch-O.D. steel boot plate. These piles were being installed using a Delmag D19-42 single-acting diesel hammer, having a manufacturer’s indicated ram weight of 4.19 kips, a manufacturer’s indicated maximum stroke of 10.25 feet, and a manufacturer’s maximum rated energy of 42.8 foot-kips.

Experience indicating that higher-capacity pile foundation systems generally have lower support costs than lower-capacity pile foundation systems notwithstanding, the stratified nature of the 12.75-inch piles’ long-term capacity distribution (long-term capacity vs. depth, as presented in Figure 12) prompted consideration of using shorter, lower-capacity 10.75-inch-O.D. piles (terminating in a suitably shallow, suitably thick competent layer) instead of longer, higher-capacity 12.75-inch-O.D. piles. To aid in comparing support costs of shorter, lower-capacity 10.75-inch piles to longer, higher-capacity 12.75-inch piles, the pile test program results were used to

estimate 10.75-inch piles' long-term capacity distribution.

To develop an EOID capacity distribution for 10.75-inch piles based on 12.75-inch data, and based on CAPWAP results, toe resistance was assumed to account for 75 percent of EOID capacity at all elevations. Using this 75/25 percent division between toe and shaft resistance, and accounting for the different toe and shaft areas of the two pile diameters, yields an estimated 10.75-inch EOID capacity distribution equal to 75 percent of the 12.75-inch average EOID capacity distribution. The estimated 10.75-inch piles' EOID capacity distribution is presented in Figure 13.

Since literature indicates that larger-diameter piles take longer to set-up than smaller-diameter piles, to estimate cumulative set-up for 10.75-inch piles based on 12.75-inch pile data, it was assumed that at a minimum the 10.75-inch piles would experience (long-term) the test-program-determined unit set-up exhibited by the 12.75-inch piles. The unit set-up determined for 12.75-inch test piles, applied to a 10.75-inch pile's surface area, results in the estimated cumulative set-up presented in Figure 13. The EOID capacity distribution and cumulative set-up so estimated for 10.75-inch piles were added together to yield estimated long-term capacity as presented in Figure 13.

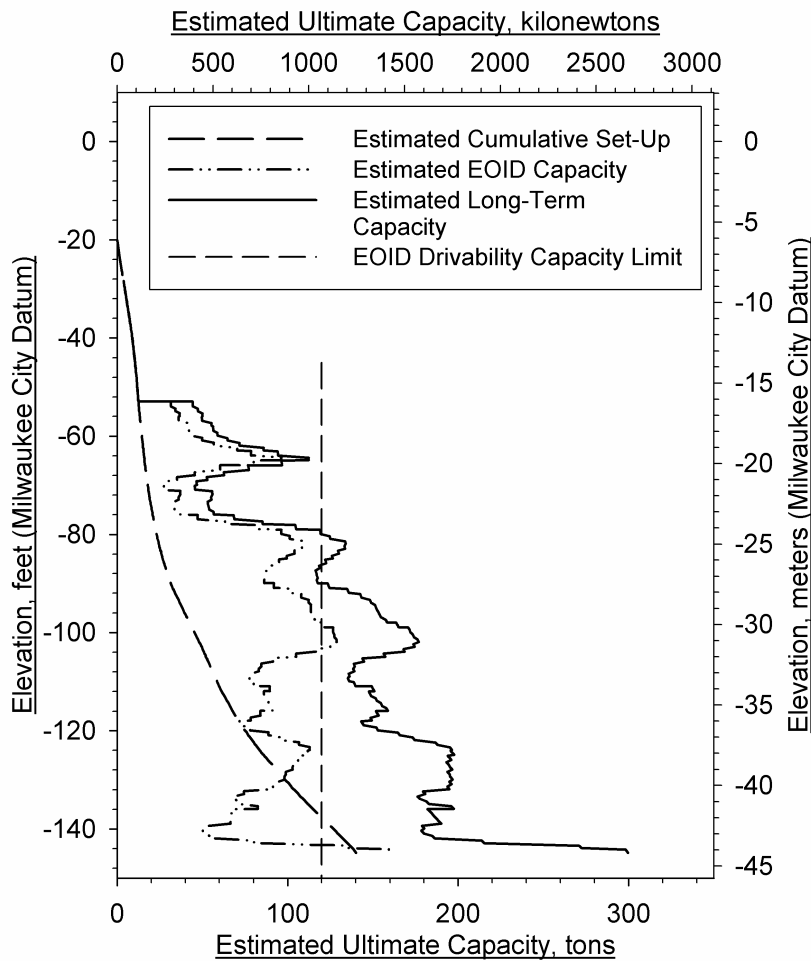


**FIG. 13. Estimated capacity vs. elevation
Delmag D19-42—10.75-inch pipe pile.**

GRLWEAP was used to predict that 10.75-inch-O.D. pipe piles, with 0.250-inch-thick walls, installed using a Delmag D19-42 at maximum anticipated stroke, would have an EOID capacity of approximately 120 tons at practical refusal (10 blows per inch (bpi)). This 120-ton EOID capacity associated with that hammer/pile combination's drivability limit is illustrated on Figure 13. A review of Figure 13 indicates that estimated EOID capacity first reaches 120 tons at approximate Elevation -98 feet; it was considered improbable that 10.75-inch piles would penetrate below this elevation. A review of Figure 13 indicates that at Elevation -98 feet, cumulative set-up is estimated to be 42 tons, resulting in an anticipated maximum long-term capacity of 162 tons, and a maximum allowable load of 81 tons.

Cost Components for Production Piles

To aid in selecting production pile size and allowable load, it was desired to evaluate the two pile sizes' relative cost-effectiveness using support cost. To calculate support cost, both allowable load and installed cost must be determined. Achievable allowable loads are the long-term capacity distributions (presented in Figures 11 and 13) divided by an appropriate factor of safety. In this case, allowable loads were determined by applying a factor of safety of 2.0 both pile sizes' long-term capacity distributions.

To evaluate specific potential combinations of pile size, capacity, depth, and cost would require determination of all these parameters at a given toe elevation. Rather than determine costs for discrete toe elevations, it was desired to characterize costs for individual production driving components as functions of toe elevation (i.e., to develop production pile cost component distributions) for both pile sizes. The contractor, Zenith Tech, Inc. of Waukesha, Wisconsin, provided cost information for individual production driving components for both pile sizes; labor, overhead, and profit were included in the costs provided. The individual component's cost distributions were added together to produce a total installed cost distribution (total installed cost vs. toe elevation) for both pile sizes. Individual cost components are discussed in the subsequent sections, and presented for 12.75- and 10.75-inch piles in Figures 14 and 15, respectively.

Pick and Move Time

This cost reflects the estimated time required to pick up a pile's bottom section, move into position, and prepare to drive. This is a fixed cost per pile, and so is independent of toe elevation (i.e., is a straight vertical line in Figures 14 and 15).

Drive Time

This cost reflects the estimated drive time required to install a pile. The estimated drive time is based on anticipated hammer blow rates, and penetration resistances evidenced in the pile test program. For any given depth interval, this cost increases with increasing average penetration resistance, and cumulatively increases with decreasing toe elevation (embedment depth).

Splices

This cost reflects the estimated time required to perform a splice. Sixty-foot-long pile sections were anticipated, and splices were modeled as accomplished with a full-penetration groove weld using a backup ring. With friction splices (not used on this project), this component would also include material cost. This cost is fixed between splice elevations, and so is a step-function with respect to toe elevation.

Pile Shell and Concrete Fill

This cost reflects the installed pile's material cost, including the steel pile shell and concrete fill. This cost increases linearly with decreasing toe elevation (embedment depth).

Waste Material

This cost reflects the waste material value for each pile installation. The south bascule bridge north pier piles were installed inside a steel sheet pile cofferdam in the South Menomonee Canal. Prior to dewatering, the inside of the cofferdam was excavated by clam bucket to subgrade elevation, the piles were installed through standing water, and a concrete seal was placed. Subsequent to dewatering, the pile stick-ups were cut off and considered waste material. The waste length for each pile, which extended from the top of the concrete seal to a workable stick-up distance above the driving template, was determined to be 24.6 feet. This is a fixed cost per pile, and so is independent of toe elevation (i.e., is a straight vertical line in Figures 14 and 15).

Crane Platform

This cost is applicable to only 12.75-inch piles, and reflects the cost of constructing an additional crane platform for a second crane location. Using a Delmag D19-42 to install 10.75-inch piles, the crane had sufficient boom radius to drive all the pier piles from one crane platform. Using a heavier Delmag D30-32 to install heavier 12.75-inch piles, the crane had insufficient boom radius to drive all the pier piles from one crane platform, requiring a second platform. This cost is independent of both toe elevation and allowable pile load, and therefore was distributed among the north pier's total supported tons. Accordingly, the additional crane platform cost was divided by the total tons supported in the north pier, and a resulting crane platform support cost increment of \$2.06 per allowable ton was uniformly added, full-depth, to the 12.75-inch support cost distribution (discussed subsequently).

Bridge Pier

For a conventional pile cap, cap cost should be included when evaluating support cost, and for a given column load, cap support cost is function of allowable pile load. Fewer higher-allowable-load piles generally result in a smaller pile cap and lower cap support cost than more lower-allowable-load piles in a larger cap. For this project, the size of the south bascule bridge north pier was fixed (i.e., independent of

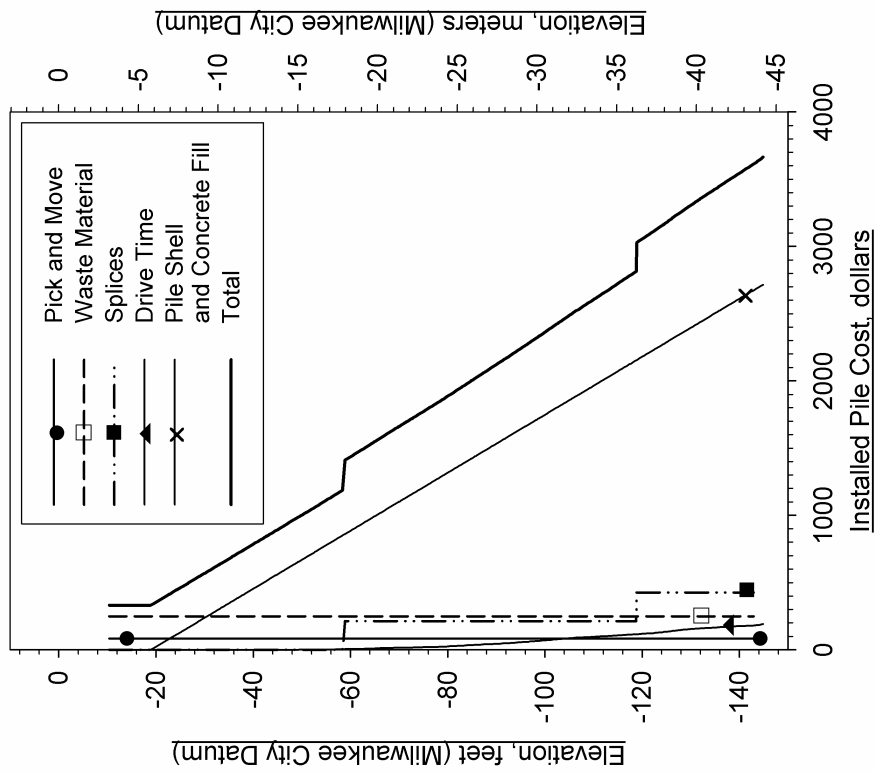


**FIG. 14. Production pile cost vs. elevation
Delmag D30-4-32—12.75-inch pipe pile.**

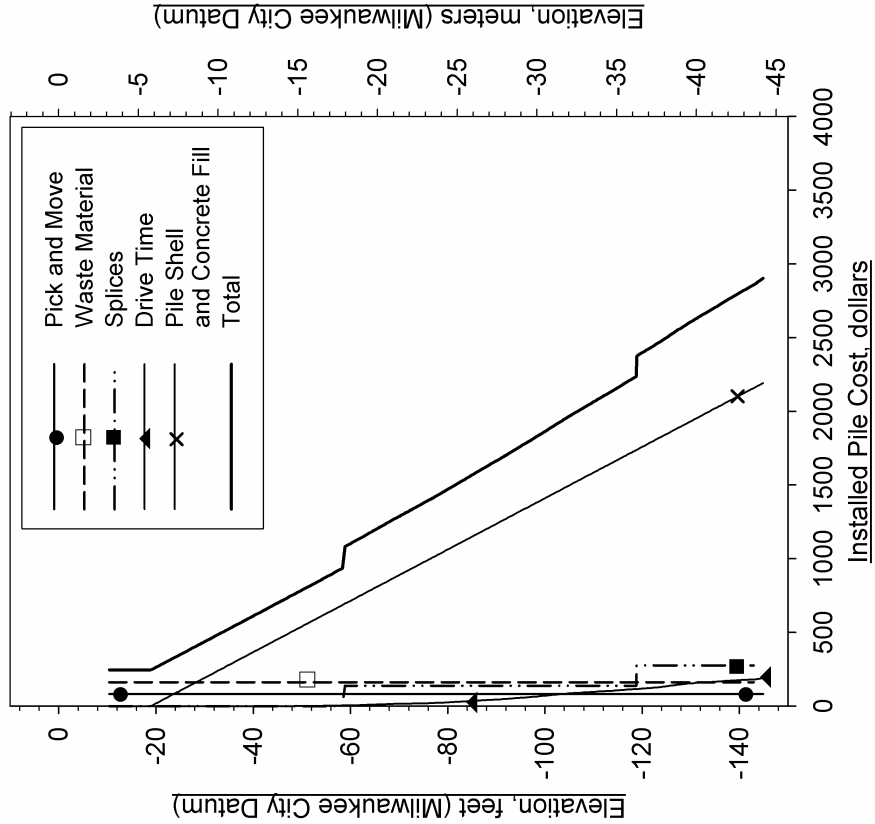


**FIG. 15. Production pile cost vs. elevation
Delmag D19-42—10.75-inch pipe pile.**

allowable pile load). Accordingly, the pier support cost was independent of both allowable load and pile size, and so was ignored in this evaluation.

Total Installed Cost Distribution

The individual cost component distributions were added together to produce a total installed cost distribution for both pile sizes. The total installed cost distributions for 12.75- and 10.75-inch piles are presented in Figures 14 and 15, respectively. A review of Figures 14 and 15 indicates that the most-significant cost component (by far) is the pile shell and concrete fill (material costs).

Support Cost Distributions

Long-term capacity is a function of elevation. Allowable load is long-term capacity divided by a factor of safety, and so is also a function of elevation. As demonstrated in the preceding sections, installed cost can also be characterized as a function of elevation. Since pile support cost is installed cost divided by allowable load, and both installed cost and allowable load are functions of elevation, pile support cost is also a function of elevation. The pile support cost distribution (pile support cost as a function of elevation) for 12.75-inch piles was determined by dividing the total production pile cost distribution presented in Figure 14 by the estimated allowable load distribution (the long-term capacity distribution presented in Figure 12 divided by a factor of safety of 2.0). To account for the cost of the additional crane platform required for installation of 12.75-inch piles, a cost increment of \$2.06 per allowable ton was uniformly added to the resulting 12.75-inch pile support cost distribution (i.e., the calculated pile support cost distribution was shifted \$2.06 per allowable ton to the right).

The pile support cost distribution for 10.75-inch piles was determined by dividing the total production pile cost distribution presented in Figure 15 by the estimated allowable load distribution (the long-term capacity distribution presented in Figure 13 divided by a factor of safety of 2.0). Recalling that it was considered improbable that 10.75-inch piles would penetrate below Elevation -98, their calculated support cost distribution was ignored (is not presented) below that elevation. The resulting pile support cost distributions for both pile sizes are presented in Figure 16.

A review of Figure 16 indicates that for this project, the two pile sizes' pile support cost distributions differ virtually by only the additional crane platform cost (i.e., without the additional crane platform cost, the two pile sizes' pile support cost distributions would have been virtually identical). This indicates that in this case, at virtually all elevations, the 12.75-inch pile's increased capacity was almost exactly offset by its increased cost. For other projects' combinations of viable pile sections' capacity and cost distributions, pile support cost distributions may exhibit greater variability.

A review of Figure 16 indicates that, with one exception, because of the 12.75-inch piles' additional crane platform cost, 10.75-inch piles exhibit lower pile support costs at all capacities and elevations. The exception occurs at approximate Elevation -145 feet, where 12.75-inch piles could achieve a long-term capacity of 400 tons, resulting in an allowable load of 200 tons. However, based on pile geometry

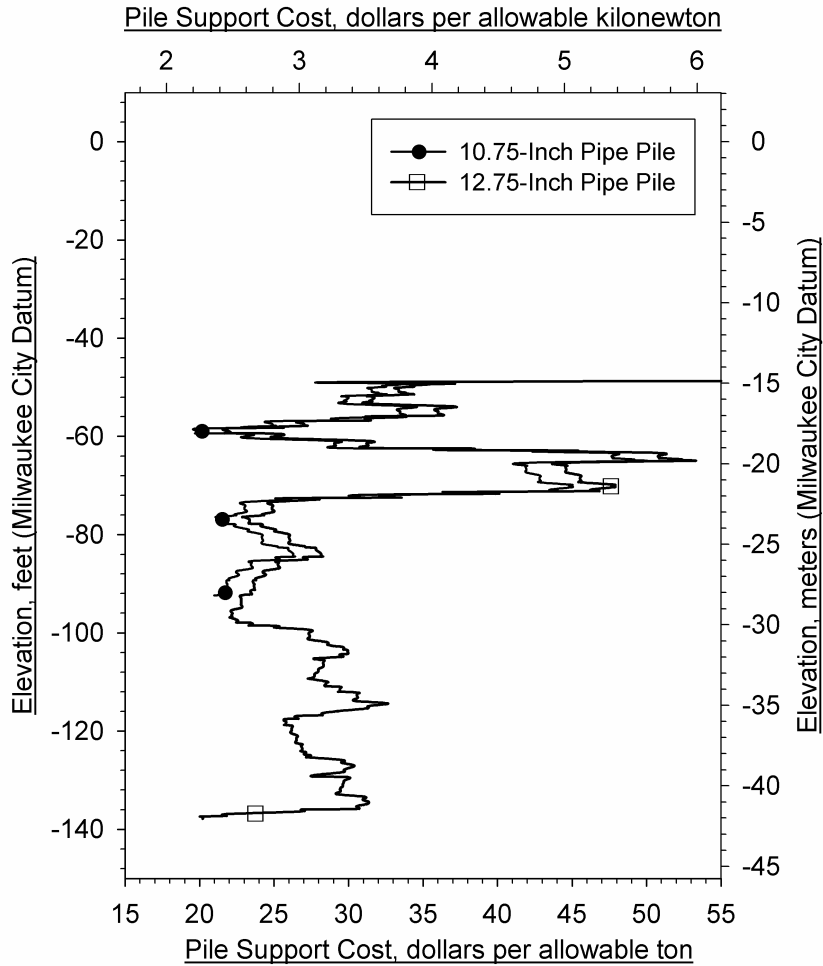


FIG. 16. Pile support cost vs. elevation.

and pier reinforcing requirements, and a required minimum number of piles to resist lateral loads, 200-ton piles were not considered viable for the structure.

The lowest 10.75-inch pile support cost (\$19.89 per allowable ton) occurs at approximate Elevation -64 feet. As evidenced in Figure 16, and confirmed by a review of Figure 13, the relatively competent layer contributing to increased capacity and decreased support cost at that elevation is rather thin, and the probability of production piles consistently terminating in that layer was considered low.

The two next-lowest 10.75-inch pile support costs are nearly equal (approximately \$21 per allowable ton), occurring at Elevations -81 and -98 feet. The shallower (Elevation -81 feet) was selected for design. A review of Figure 13 indicates that at Elevation -81 feet, long-term capacity was anticipated to be on the order of 125 tons. Based on this evaluation of the pile support cost distributions, and incorporating a factor of safety of 2.0, it was recommended that the south bascule bridge north pier be supported by 10.75-inch piles having an allowable load of 60 tons (installed to a long-term capacity of 120 tons).

Production-Pile Installations

Based on pile/pier load and geometry considerations, the designer selected an allowable load of 65 tons for the north pier piles, resulting in a required long-term capacity of 130 tons. A review of Figure 13 indicates that 10.75-inch piles could be expected to develop a long-term capacity of 130 tons at approximate Elevation -82 feet. However, at approximate Elevation -82 feet, the anticipated long-term capacity only marginally exceeds 130 tons, and decreases below. Slight variability in subsurface conditions, and/or slight conservatism in production-pile penetration resistance criteria, could be expected to result in production piles terminating below Elevation -82 feet. A review of Figure 13 indicates that if the piles extend below Elevation -82 feet, they could next be expected to develop a long-term capacity of 130 tons at approximate Elevation -91 feet.

Similar to as presented in the first case history, the cumulative set-up for 10.75-inch-O.D. pipe piles presented in Figure 13 was used to develop depth-variable production-pile penetration resistance criteria. The south bascule bridge north pier 65-ton (allowable load) production piles had an average embedded depth of 74 feet, corresponding to an average toe elevation of -94 feet. This indicates that on average, the piles indeed extended beyond Elevation -82 feet, and the actual average toe elevation compares well with an estimated toe elevation of -91 feet in this eventuality. A review of Figure 16 indicates that this likely resulted in only slightly higher pile support costs (approximately \$1 per allowable ton) than had the piles terminated at Elevation -82 feet.

CONCLUSIONS

- Set-up can account for a significant portion of long-term pile capacity. For the first case history presented, set-up accounts for up to 71 percent of long-term capacity. Accounting for set-up in pile design offers numerous benefits, and can result in using smaller hammers, smaller pile sections, shorter piles, higher capacities, and more-economical installations (lower pile support costs) than otherwise possible.
- The characterization not only of set-up magnitude, but also of set-up distribution, offers design- and construction-phase advantages, such as developing depth-variable installation criteria which incorporate set-up for numerous different required production-pile capacities, and more-accurate assignment of reduced capacities to short or damaged piles.
- Dynamic monitoring at both EOID and BOR, combined with subsequent CAPWAP analyses, allows determination of both set-up magnitude and distribution. Subtraction of CAPWAP-determined EOID shaft resistance distribution from CAPWAP-determined BOR shaft resistance distribution allows determination of set-up distribution. Whether or not full capacity is mobilized at EOID and/or at BOR, and the associated effects on calculated set-up distributions, should be recognized and accounted for in selecting a design set-up distribution, and in selecting potential allowable production-pile loads.
- Since set-up is predominately a shaft-resistance phenomenon, and since residual stress and non-residual stress CAPWAP analyses can result in different shaft

resistance predictions, the type of analyses (i.e., residual vs. non-residual) used to determine set-up distribution should be the same for both EOID and BOR analyses.

- Piles exhibiting differing driving behavior can exhibit similar set-up distributions.
- Initial-drive dynamic monitoring results, combined with set-up distributions, can be used to predict piles' long-term capacities as functions of depth. This information can prove useful when evaluating potential production-pile sections, and allowable loads.
- Support cost provides a normalized cost-effectiveness measure of a foundation system, and affords direct "apples-to-apples" economic comparison between viable foundation alternatives.
- Production pile installation costs can be separated into components. These cost components can be expressed as functions of toe elevation/depth and summed, yielding total installed pile cost distributions. For the second case history presented, and likely for most projects, material cost is the predominate pile cost component. For the second case history presented, drive time was a relatively insignificant cost component. For other soil profiles requiring significant length of pile penetration through more-competent layers, drive time may account for greater contribution to installed pile cost.
- Pile cost distributions can be divided by pile capacity distributions to yield pile support cost distributions. The use of pile support cost distributions is applicable in all soil profiles, accounts for subsurface stratigraphy, and allows normalized economic comparison to aid selecting the most-cost-effective viable pile type, section, and capacity.

ACKNOWLEDGEMENTS

The introductory set-up discussion presented herein is based partly on research funded by the Wisconsin Department of Transportation and the United States Department of Transportation in the interest of information exchange, and is the result of research done under the auspices of the Department and the Wisconsin Highway Research Program.

APPENDIX I. CONVERSION TO SI UNITS

1 inch (in) = 2.540×10^{-2} meters (m)

1 foot (ft) = 0.3048 meters

1 foot-kip (ft-kip) = 1.356×10^3 newton-meters (N-m)

1 kip = 4.448×10^3 Newtons (N)

1 kip per square inch (ksi) = 6.895 megapascals (MPa)

1 pound per square foot (psf) = 47.88 pascals

1 pound per square inch (psi) = 6.895×10^3 pascals

1 U.S. ton = 8.896×10^3 newtons

1 U.S. ton per square foot (tsf) = 95.76×10^3 pascals

REFERENCES

- Bullock, Paul Joseph (1999). "Pile Friction Freeze: A Field and Laboratory Study, Volume 1," Ph.D. Dissertation, University of Florida.
- Camp III, William M., Wright, William B., and Hussein, Mohamad (1993). "The Effect of Overburden of Pile Capacity in a Calcareous Marl," *Deep Foundations Institute 18th Annual Members' Conference*, pp.23-32.
- Camp III, W.M., and Parmar, H.S. (1999). "Characterization of Pile Capacity with Time in the Cooper Marl: A Study of the Applicability of a Past Approach To Predict Long-Term Pile Capacity," *Emre, TRB*, pp. 1-19.
- Chow, F.C., R.J. Jardine, J.F. Nauroy, and F. Brucy (1997). "Time-related Increase in Shaft Capacities of Driven Piles in Sand," *Géotechnique*, Vol. 47, No. 2, pp. 353-361.
- Chow, F.C., Jardine, R.J., Brucy, F., and Nauroy, J.F. (1998). "Effects of Time on Capacity of Pipe Piles in Dense Marine Sand," *Journal of Geotechnical and Geoenvironmental Engineering*, Vol. 124, No. 3, ASCE, pp. 254-264.
- Davisson, M.T. (1973). "High Capacity Piles," *Innovations in Foundation Construction; Proceeding of ASCE Illinois Section and Illinois Institute of Technology Lecture Series, January 19, 1982 – May 3, 1982*, pp. 81-112.
- Fellenius, Bengt H., Brusey, Walter G., and Pepe, Frank (2000). "Soil Set-up, Variable Concrete Modulus, and Residual Load for Tapered Instrumented Piles in Sand," *Specialty Conference on Performance Confirmation of Constructed Geotechnical Facilities*, University of Massachusetts, Amherst, April 9-12, 2000, ASCE, pp.1-17.
- Fellenius, Bengt H. (2001a). "From Strain Measurements to Load in an Instrumented Pile," *Geotechnical News Magazine*, Vol. 19, No. 1, pp. 35-38.
- Fellenius, Bengt H. (2001b). "Determining the Resistance Distribution in Piles. Part 1: Notes on Shift of No-Load Reading and Residual Load," *Geotechnical News Magazine*, Vol. 20, No. 2.
- Fellenius, Bengt H. (2001c). "Determining the Resistance Distribution in Piles. Part 1: Method for Determining the Residual Load," *Geotechnical News Magazine*, Vol. 20, No. 3.
- Fellenius, Bengt H. (2002). "Determining the True Distributions of Load in Instrumented Piles," *Proc., International Deep Foundations Congress 2002*, Geotechnical Special Publication No. 116, Vol. 2, ASCE, pp.1455-1470.
- Finno, Richard J., Achille, Jacques, Chen, Hsin-Chin, Cosmao, Tanguy, Park, Jun Boum, Picard, Jean-Noel, Smith D. Leeanne, and Williams, Gustavious P. (1989). "Summary of Pile Capacity Predictions and Comparison With Observed Behavior," *Predicted and Observed Axial Behavior of Piles*, Geotechnical Special Publication No. 23, ASCE, pp. 356-385.
- Finno, Richard J., Cosmao, Tanguy, and Gitskin, Brett (1989). "Results of Foundation Engineering Congress Pile Load Tests," *Predicted and Observed Axial Behavior of Piles*, Geotechnical Special Publication No. 23, ASCE, pp. 338-355.
- Giles Engineering Associates, Inc., "Geotechnical Engineering Exploration and Preliminary Analysis – Proposed 6th Street Viaduct Reconstruction, 6th Street

- (Clybourn Street to Virginia Street) Milwaukee, Wisconsin,” prepared for Earth Tech c/o City of Milwaukee, May 24, 2000, Giles Project No. 1G-0004048.
- Goble, George G., Likins, Garland E., and Rausche, Frank (1975). “Bearing Capacity of Piles from Dynamic Measurements,” Final Report, Department of Civil Engineering, Case Western Reserve University, Cleveland, Ohio.
- Guang-Yu, Z. (1988). “Wave Equation Applications for Piles in Soft Ground,” *Proc., 3rd International Conference on the Application of Stress-Wave Theory to Piles* (B. H. Fellenius, ed.), Ottawa, Ontario, Canada, pp. 831-836.
- Hannigan, Patrick J., Goble, George G., Thendean, G., Likins, George E., and Rausche, Frank (1997). *Design and Construction of Driven Pile Foundations – Volume II*, Federal Highway Administration Report No. FHWA-HI-97-013.
- Huang, S. (1988). “Application of Dynamic Measurement on Long H-Pile Driven into Soft Ground in Shanghai,” *Proc., 3rd International Conference on the Application of Stress-Wave Theory to Piles* (B. H. Fellenius, ed.), Ottawa, Ontario, Canada, pp. 635-643.
- Hussein, Mohamad, and Rausche, Frank (1988). “Wave Equation Analysis of Pile Driving: Methodology and Performance,” *Proc., ASCE’s 6th National Conference on Microcomputers in Civil Engineering*, November 9-11, Orlando, Florida.
- Hussein, Mohamad, and Likins, Garland E. (1995). “Dynamic Testing of Pile Foundations During Construction,” *Proc., ASCE Structures Congress XIII*, Boston, Massachusetts.
- Hussein, Mohamad, Sharp, Mike, and Knight, William (2002). “The Use of Superposition for Evaluating Pile Capacity,” *Proc., ASCE_GeoInstitutes’s International Deep Foundation Congress*, Orlando, Florida.
- Komurka, Van E., Wagner, Alan B., and Edil, Tuncer B. (2003a). “A Review of Pile Set-Up,” *Proc., 51st Annual Geotechnical Engineering Conference*, University of Minnesota, St. Paul, Minnesota, February 21, 2003.
- Komurka, Van E., Wagner, Alan B., and Edil, Tuncer B. (2003b). “Estimating Soil/Pile Set-up,” Wisconsin Highway Research Program Contract No. 0092-00-14, Report No. 0305, September 2003.
- Likins, Garland E., Rausche, Frank, Thendean, Gabriel, and Svinkin, Mark (1996). “CAPWAP Correlation Studies,” STRESSWAVE’96 Conference, Orlando, Florida
- Likins, Garland E., Rausche, Frank, and Goble, George G. (2000). “High Strain Dynamic Pile Testing, Equipment and Practice,” *Proc., Sixth International Conference on the Application of Stress-Wave Theory to Piles*, São Paulo, Brazil, September 11-13, 2000.
- Long, James H., Kerrigan, John A., and Wysockey, Michael H. (1999). “Measured Time Effects for Axial Capacity of Driven Piling,” *Transportation Research Record 1663*, Paper No. 99-1183, pp.8-15.
- Lukas, Robert G., and Bushell, Ted D. (1989). “Contribution of Soil Freeze to Pile Capacity,” *Foundation Engineering: Current Principles and Practices*, Vol. 2, ASCE, pp 991-1001.
- Malhotra, S. (2002). “Axial Load Capacity of Pipe Piles in Sand: Revisited,”

- Deep Foundations Congress, Geotechnical Special Publication*, No 116, Vol. 2, ASCE, Reston, Va., pp 1230-1246.
- McVay, M.C., Schmertmann, J., Townsend, F., and Bullock, P. (1999). "Pile Friction Freeze: A Field and Laboratory Study," *Florida Department of Transportation*, Vol. 1, pp.192-195.
- Pile Dynamics, Inc. (1998). *Pile Driving Analyzer Manual, Model PAK*, Cleveland, Ohio.
- Randolph, M.F., Carter, J.P., and Wroth, C.P. (1979). "Driven Piles in Clay – the Effects of Installation and Subsequent Consolidation," *Géotechnique* 29, No. 4, pp. 361-393.
- Rausche, Frank, Goble, George G., and Moses, F. (1972). "Soil Resistance Predictions from Pile Dynamics," *Journal of the Soil Mechanics and Foundations Division*, Vol. 98, No. SM9, September 1972, ASCE, pp.917-937.
- Rausche, Frank, Goble, George G., and Likins, Garland E. (1985). "Dynamic Determination of Pile Capacity," *Journal of Geotechnical Engineering*, Vol. 111, No. 3, ASCE, pp367-383.
- Rausche, Frank, Hussein, Mohamad, Likins, Garland E., and Thendean, Gabriel (1994). "Static Pile Load-Movement from Dynamic Measurements," *Proc., ASCE Geotechnical Engineering Division's Vertical and Horizontal Deformations of Foundations and Embankments Conference*, College Station, Texas.
- Rausche, Frank, Richardson, B., and Likings, Garland E. (1996). "Multiple Blow CAPWAP Analysis of Pile Dynamic Records," *STRESSWAVE'96 Conference*, Orland. Florida.
- Rausche, Frank, Robinson, B., and Liang, L. (2000). "Automatic Signal Matching with CAPWAP," *Proc., Sixth International Conference on the Application of Stress-Wave Theory to Piles*, São Paulo, Brazil, September 11-13, 2000.
- Samson, L., and Authier, J. (1986). "Change in pile capacity with time: Case histories," *Canadian Geotech. Journal*, 23(1), pp. 174-180.
- Schmertmann, John H. (1981). "A General Time-Related Soil Friction Increase Phenomenon," *Laboratory Shear Strength of Soil, ASTM STP 740*, R.N. Yong and F.C. Townsend, Eds., American Society for Testing and Materials, pp. 456-484.
- Schmertmann, John H. (1991). "The Mechanical Aging of Soils," *Journal of Geotechnical Engineering*, Vol. 117, No. 9, September 1991, ASCE, pp.1288-1330.
- Seed, H.B., and Reese, L.C. (1955). "The Action of Soft Clay Along Friction Piles," *Proceedings of the American Society of Civil Engineers* 81, Paper 842.
- Skov, Rikard, and Denver, Hans (1988). "Time-Dependence of Bearing Capacity of Piles," *Proceedings 3rd International Conference on Application of Stress-Waves to Piles*, pp. 1-10.
- Soderberg, Lars O. (1961). "Consolidation Theory Applied to Foundation Pile Time Effects," *Géotechnique*, London, Vol. 11, No. 3, pp. 217-225.
- STS Consultants, Ltd., "Subsurface Exploration and Preliminary Geotechnical Engineering Evaluation for the Proposed Sixth Street Viaduct Replacement Project in Milwaukee, Wisconsin," prepared for Earth Tech, April 23, 1999, STS Project No. 85180.

- Svinkin, Mark R. (1996). "Setup and Relaxation in Glacial Sand – Discussion," *Journal of Geotechnical Engineering*, Vol. 122, No. 4, ASCE, pp. 319-321.
- Svinkin, Mark R., Skov R. (2000). "Set-Up Effect of Cohesive Soils in Pile Capacity," *Proceedings, 6th International Conference on Application of Stress Waves to Piles*, Sao Paulo, Brazil, Balkema, pp. 107-111.
- Thendean, G., Rausche, Frank, Svinkin, Mark, and Likins, Garland E. (1996). "Combining Static Pile Design and Dynamic Installation Analysis in GRLWEAP," STRESSWAVE'96 Conference, Orlando, Florida.
- Titi, Hani H., and Wathugala, G. Wije (1999). "Numerical Procedure for Predicting Pile Capacity – Setup/Freeze," *Transportation Research Record 1663*, Paper No. 99-0942, pp. 25-32
- Wang, Shin-Tower, and Reese, Lymon C. (1989). "Predictions of Response of Piles to Axial Loading," *Predicted and Observed Axial Behavior of Piles*, Geotechnical Special Publication No. 23, ASCE, pp. 173-187.

KEY WORDS

Dynamic monitoring, dynamic testing, PDA testing, pile capacity, pile design, Pile Driving Analyzer (PDA), pile set-up, pile support cost, piles, pile testing, set-up, support cost.